

BULK SUPERCONDUCTIVITY ON OZONE ANNEALED YBCO SAMPLES BY A.C. SCREENING CURRENT MEASUREMENTS

F. CELANI and A. SAGGESE

INFN - Laboratori Nazionali Frascati, Frascati (Italy)

S. PACE and L. LIBERATORI

Dipartimento di fisica, Universita' di Salerno, Salerno (Italy)

N. SPARVIERI

Selenia Spa Direzione Ricerche, Rome (Italy)

Received September 1, 1989; accepted October 3, 1989

ABSTRACT

Sintered samples of $Y_1Ba_2Cu_3O_{7-\delta}$ prepared with a modified citrate pyrolysis and annealed in an ozone atmosphere are tested with a.c. screening current in a geometrical configuration able to detect a true bulk superconductivity. A picture of the main features of diamagnetic behaviour of sintered high T_c superconductors is given to explain the a.c. susceptibility measurements in such materials. Comparisons among samples respectively annealed with and without ozone atmosphere have been performed as a function of the amplitude of the a.c. magnetic field. At small fields ozone samples just 2K below the superconducting transition temperature have a complete shielding while, with the same a.c. magnetic field, oxygen samples show the complete shielding at lower temperature. For samples with simple geometrical shape the absolute reference, corresponding to the 100 % shielding is obtained by using Nb or Pb superconducting samples with identical shapes. In the absence of an absolute reference for arbitrary shapes, the complete diamagnetic shielding can be inferred by the absence of the frequency dependence in the a.c. susceptibility. Such analysis clearly shows the better quality of the ozone samples.

INTRODUCTION

In any preparation method of sintered high - T_c superconducting oxides, the determination of the real volume superconducting percentage should be of fundamental interest. Otherwise, sometimes, such tests are not performed in detail, leading to an uncertain meaning of bulk and surface measured properties. In fact, a 15 - 20 % volume superconductivity allows the presence of superconducting paths which may simulate a complete sample superconductivity by resistive measurements. On the

contrary the diamagnetic measurements can be related to volume properties. Nevertheless some care is needed for a correct interpretation of the susceptibility measurements. For this reason the following section is devoted to a brief discussion of the diamagnetic behaviour of granular superconductors and summarises the main characteristics of magnetization curves [1]. From this picture a description of the magnetic a.c. susceptibility behaviour as a function of temperature and amplitude of the a.c. magnetic field is recalled. In particular, agreeing with McCallum et al., [2] we believe that the frequency dependence of the screening currents for frequency up to tens of KHz can clearly detect the presence of normal phases inside the sintered pellets.

Because we developed a new $Y_1Ba_2Cu_3O_{7-\delta}$ fabrication method which uses a modified citrate pyrolysis followed by an annealing in ozone enriched oxygen mixture, it is very important for us to set up a simple method which allows to determine the amount of superconducting phase and the grain coupling strength in our pellets. The key points of the preparation method and the experimental apparatus for measuring the frequency dependence of the magnetic susceptibility are described later. This apparatus in spite of its simplicity allows to preserve a good signal to noise ratio also in experimentally adverse conditions like low frequencies and weak measuring magnetic fields. The analysis of the experimental data is then reported.

Such measures together with resistive measurements, obtained by the four probe method, constitute the first step before a full characterization using more complex experimental apparatus. Nevertheless the comparison between samples made with or without ozone, shows that the ozone determines an improvement of all diamagnetic properties.

MAGNETIZATION AND MAGNETIC SUSCEPTIBILITY

As well known the diamagnetic behaviour of high - T_c sintered superconductors is complex and guided by many factors:

- a) the anisotropy of all critical fields caused by the material intrinsic structural anisotropy,
- b) the granular structure of the sintered samples which behave as an ensemble of weakly coupled superconducting domains.

The granular structure is hierarchic i.e. the grains have a granular sub - structure made of smaller weakly coupled crystals. Moreover the crystals rarely behave as true single crystals, but they can be considered as a set of coupled monocrystals. For simplicity these structures are neglected and the whole system is described by a single level granular structure without internal anisotropy. The main elements which determine the diamagnetic behaviour of sintered samples are:

- 1) grain coupling, which is characterized by the coupling strength and the dimensions and number of coupled domains.
- 2) intergranular non superconducting regions (vacuum, metallic, semiconducting, insulating) of whom both dimensions and number are relevant.

Of course, in a quantitative analysis, the random distribution of these parameters should be taken into account, but for a first qualitative approach these distributions can be neglected assuming the system is completely homogeneous.

Grain coupling

The grain coupling is usually described using Josephson junctions characterized by the Josephson penetration depth λ_J [3]. Such depth λ_J is proportional to the inverse of the root of the maximum superconducting current density between grains i.e. $\lambda_J \simeq 1/\sqrt{J_J}$; where the current density J_J is proportional to the tunnel probability between grains, so that J_J can be taken as a measure of the coupling strength.

For a single junction, λ_J determines the distances in which current and magnetic field variations occur. Into a granular system the whole coupling is given by a large number of junctions separated from each other by uncoupling regions. This coupling determines the critical current density of the macroscopic transport current \bar{J}_C which can be obviously much smaller than the intrinsic critical current in the grains. Indeed the density of the critical current \bar{J}_C is determined both by J_J and by the ratio between coupling and uncoupling surfaces. In the intergranular regions the mean magnetic field falls only because of the coupling regions where J_J flows, so that an effective penetration depth $\lambda_{eff} > \lambda_J$ can be introduced. Since λ_{eff} determines the penetration depth of the magnetic field only in the intergranular regions, in case of non negligible magnetic field any single grain is shielded by superconducting currents over the London penetration depth λ_L on the grain surface.

For a single junction the maximum value of the Josephson superconducting current I_J is a function of the applied magnetic field and depends on the ratio between the junction dimensions and λ_J , but in any case the increase of the applied magnetic field reduces the mean value of I_J [3,4]. Moreover the granular system behaves as an interferometer network. As well known for a single interferometer the maximum of the superconducting current is modulated by the magnetic flux linked into the device, so that in the sintered pellet the superconducting current will depend on the magnetic flux trapped into the intergranular regions between coupled grains.

As the magnetic field increases these phenomena determine a fast decrease of the mean value of the superconducting critical current density \bar{J}_C of the sample. The decreasing rate will be, not a function of the coupling strength, but a function of both the junction and intergranular region dimensions. The decrease of \bar{J}_C will lead to an increase of λ_{eff} . Only in case of $\lambda_{eff}(H)$ greater than the sample dimensions, it is possible to assume that the superconducting currents are uniformly distributed in the sample and it is correct to compute $\bar{J}_C = I_C/S$, where S is the sample section.

The decreasing of the mean coupling between grains caused by the magnetic field, in presence of both thermal fluctuations and screening currents, determines a critical field H_{C2}^G , above which the grains are completely decoupled.

Intergranular regions

The non superconducting intergranular regions are constituted both by holes, and by normal lumps of either semiconducting or insulating materials. The holes are due to a non perfect compactness of the sintered pellet, which shows a density lower than the theoretical value. The other non

superconducting volumes are generated by an incorrect local stoichiometry determined by impurities or by an inhomogeneous mixing of the components during the preparation, or by an incorrect oxygenation [5].

In the usual superconductors, because of the large value of the coherence length, analogous defects cause a decrease of the critical temperature. For superconducting oxides the very short coherence length ($\xi = 10 - 30 \text{ \AA}$) allows the defects to form non superconducting regions in the material leaving the transition temperature unchanged.

The magnetic field preferentially penetrates in the non superconducting regions where flux quanta can be trapped, so that such regions can act as pinning centers. For infinitely long cylinders, weak and non superconducting regions behave as pinning centers only if the sample is cooled in the presence of the magnetic field, or if, after a zero field cooling, a lower critical field is exceeded. For finite geometry, as shown later, the presence of holes can determine a reduction of the diamagnetic effects on the a.c. susceptibility also for external fields below this critical value.

The volume of non superconducting regions is not directly linked to the imperfect diamagnetic properties, which depend in a determinant way upon the number and dimensions of the non superconducting regions. For instance let us suppose that the sample has a large number of non superconducting cylindrical regions, each of them with a surface ξ^2 , and that the mean distance between single regions is λ_L . In this situation, if the magnetic field penetrates in the pinning centers, it will penetrate almost completely into the sample. Because in the superconducting oxides the ratio λ_L/ξ is very high (of the order of hundreds), it should be sufficient to have a fraction $1/10^4$ of the total volume made of finely divided non superconducting material to have a full field penetration. In general an incomplete magnetic field expulsion determines only an effective volume V_{eff} of non superconducting zone made of the non superconducting intergranular zone V_{int} plus a shell with thickness λ_L and volume $V_\lambda(T)$ around the intergranular regions. In a quantitative analysis the demagnetization factors of the grains should be taken into account, but in a first approximation we can write :

$$V_{\text{eff}}(T) = V_{\text{int}} + V_\lambda(T) \quad (1)$$

If $V_{\text{int}} \gg V_\lambda(T)$, as in the extreme case of non superconducting zones much larger than λ_L , the $V_{\text{eff}}(T)$ will be a very weak function of the temperature. Otherwise, in case of very fine division of non superconducting zones eqn. 1 gives :

$$V_{\text{eff}}(T) \cong V_\lambda(T) \propto \lambda_L^2(T) \quad (2)$$

A large temperature dependence of $V_{\text{eff}}(T)$ will be observed also in the case of non homogeneous material with a large transition temperature distribution, so that, independently of the magnetic field penetration depth, an intrinsic temperature dependence of $V_{\text{int}}(T)$ will appear. Only a careful measurement of the diamagnetic properties behaviour as a function of the temperature and magnetic field can lead to a quantitative determination of both $V_{\text{int}}(T)$ and $V_\lambda(T)$ without the possibility to discriminate the conducting or the nonconducting nature of the intergranular material.

On the contrary, agreeing with McCallum et al., [2], we believe that the frequency dependence of the susceptibility is a certain way to show the presence of metallic material inside a sample. Indeed, the flux variations of the magnetic field generate eddy currents in metallic intergranular regions reachable by the magnetic field. The presence of eddy currents is easily revealed by observing the frequency increase of the diamagnetic a.c. susceptibility in the superconducting state.

For a.c. susceptibility measurements, the working frequency is usually chosen such that the resistivity of the sample in the normal phase is high enough to avoid significant eddy currents. The previous condition is insufficient below T_c and just above the critical current between grains. Indeed in these conditions the grain superconductivity lowers the sample resistivity which reduces only to the coupling resistance between grains. In this way a significant frequency dependent diamagnetic signal can be generated in open large superconducting loops closed by small normal links.

An example of this phenomenon is illustrated in Fig. 1, where a superconducting ring, made of coupled grains, and its equivalent circuit are shown. In this case the inductance L and the junction resistance R_J of the weakest junction determine the frequency dependent eddy currents.

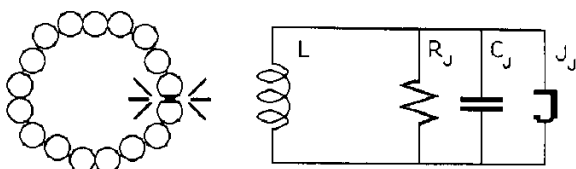


Fig. 1. Superconducting granular loop, and its equivalent circuit; L is the inductance of the loop, R_J and C_J are the resistance and the capacitance of the weakest Josephson junction between grains.

Magnetization hysteresis

The main features of magnetization hysteresis for a sintered high T_c superconductor are reported in Fig. 2. For very small magnetic fields the system will behave as a bulk superconductor with surface currents in the thickness λ_{eff} which shield the sample. Of course in case of λ_{eff} greater than the grain dimensions, currents on the grains surfaces shield the magnetic field inside the grains.

The increase of the applied magnetic field will increase the shielding current on the sample surface, until it overcomes the critical current of the weakest link between grains, so that the link becomes normal and the superconducting loop will open with a magnetic flux partial penetration. The subsequent decay of the superconducting current of the loop shall lead the superconducting loop to settle again. This phenomenon generates an entrapment of magnetic flux quanta in the intergrain regions and generates magnetization hysteresis. In this way sintered samples show a lower critical field H_{C1}^G determined by the grain coupling.

Further increase of the magnetic field will increase the amplitude of the hysteresis loops until the critical magnetic field H_{C2}^G is reached. Above this value the hysteresis disappear and the behaviour

returns to reversibility. H_{C2}^G has the same effect as an upper critical field of the intergranular regions. For fields above H_{C2}^G the magnetic field penetrates completely in the intergranular regions and the grains will be decoupled. Of course on the grain surfaces superconducting currents will shield the inner part of any single grain.

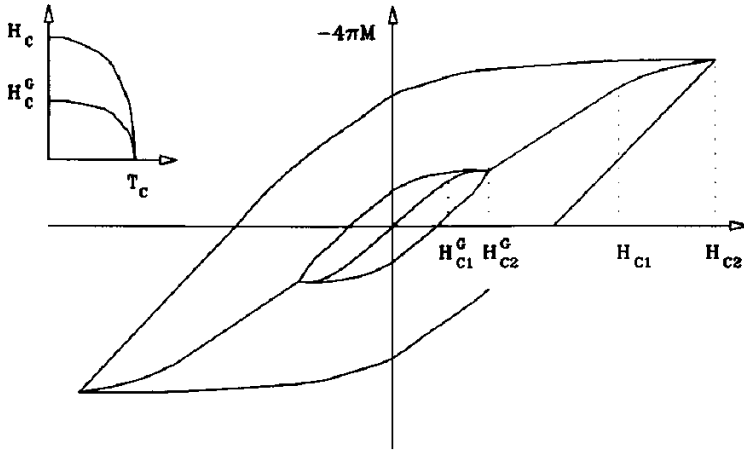


Fig. 2. Magnetization curve of granular systems; in the insert the qualitative temperature dependence of critical fields is shown.

The hysteresis effect will appear again when the applied field exceeds the true lower critical field H_{C1} of the material, so that the penetration inside the grains starts. Likewise in the usual second kind superconductors there will be a value of the magnetic field H_{C2} for which the superconductivity will be completely destroyed.

Magnetic susceptibility

As shown in the insert of Fig. 2, all critical fields have almost the same temperature dependence, so that the magnetization hystereses are functions of the temperature, and in particular they have their maximum extent at $T = 0K$ and shrink as the temperature increases.

In susceptibility measurements a temperature independent a.c. magnetic field with maximum value \bar{H}_A is applied to the sample. For a given temperature T_0 and $H_{C1}^G(T_0)$ high enough, the value of \bar{H}_A can be chosen lower than $H_{C1}^G(T_0)$ so that, at this temperature, the a.c. magnetic field penetrates only in a shell λ_{eff} of the sample volume. Neglecting the demagnetization factor, if λ_{eff} is much smaller than the sample dimensions, we have $\chi' = -1/4\pi$ and $\chi'' = 0$.

Raising the temperature, all critical magnetic fields, and in particular $H_{C1}^G(T)$, decrease until $\bar{H}_A > H_{C1}^G(T)$. At this temperature the a.c. magnetic field starts to break the intergrain junctions

and penetrates in the intergranular regions so that $|\chi'|$ decreases. The penetration of the magnetic field generates hysteresis leading $\chi'' \neq 0$. A further increase of the temperature increases the amount of broken junctions. The penetration of the magnetic field in the intergranular regions and the consequent decrease of $|\chi'|$ will saturate when $\bar{H}_A = H_{C2}^G(T)$. This temperature corresponds to a maximum of the χ'' value.

For temperatures such that $\bar{H}_A \gg H_{C2}^G$ and $\bar{H}_A \leq H_{C1}$, the sample behaves as an ensemble of disjointed grains. The χ' value corresponds to the flux expulsion for each grain with a flux penetration in the effective volume V_{eff} as given by eqn. 1. In this temperature range, because H_{C2}^G decreases as the temperature increases, if $\bar{H}_A \gg H_{C2}^G$ the hysteresis becomes almost negligible and $\chi'' \approx 0$.

Further increase of the temperature near the transition leads to $H_{C1} < \bar{H}_A < H_{C2}$, so that the grain transition is measured. The qualitative behaviour of the temperature dependence of χ' and χ'' is reported in Fig. 3.

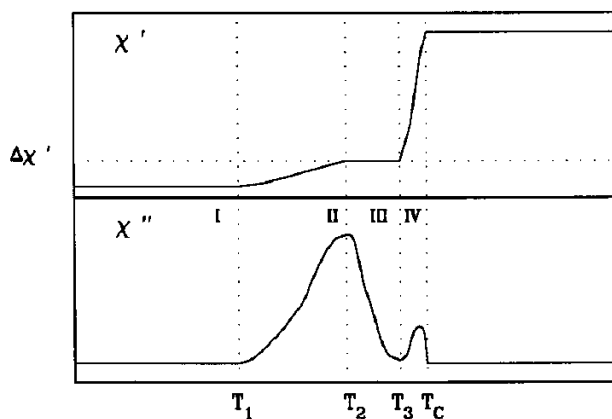


Fig. 3. Qualitative temperature dependence of χ' and χ'' ; four temperature ranges are identified: I) $\bar{H}_A < H_{C1}^G$, II) $H_{C1}^G < \bar{H}_A < H_{C2}^G$, III) $H_{C2}^G < \bar{H}_A < H_{C1}$, IV) $H_{C1} < \bar{H}_A < H_{C2}$.

The temperature range $T_c - T_3$ is smaller for samples which have better homogeneity of the material in the grains. The T_1, T_2 values are determined by the grain coupling strength, and the temperature range $T_1 - T_2$ gives information on the grain coupling homogeneity. Indeed higher values of T_1 and T_2 mean stronger couplings and a smaller $T_1 - T_2$ temperature interval reveals more uniformity on the grain couplings. Last but not least, $\Delta\chi'$ takes into account the effective volume of the intergranular materials.

PREPARATION METHOD AND EXPERIMENTAL SET-UP

High T_c superconducting peroxides can be easily prepared starting by mixing oxide and/or carbonate powders. Thermal processes with a solid state reaction and a subsequent annealing give samples in the form of sintered pellets. In these methods the poor quality of the samples is often

generated by a non homogeneous mixing of the starting components. In order to overcome this drawback, a mixing of nitrate solutions can be used. Our preparation method is an improvement of the usual pyrolytic technique recently applied to ceramic superconductors [6]. At the beginning the powders of yttrium and copper oxides and barium carbonate are dried and then weighted according to the final stoichiometry. The addition of nitric acid generates three nitrate mixtures with an excess of nitric acid. These liquids are blended and, in order to avoid nitrate precipitation, citric acid is added. The citric acid is more effective in a $\text{PH} \approx 6.7$; this condition is obtained by a slow addition of ammonia. Best control of an homogeneous component mixing is achieved by a direct optical method, observing the transition from a turbid dark blue mixture into a very clean light blue solution. This solution is heated up until it becomes a black mud that spontaneously fires (pyrolytic reaction); at the end of the reaction a very fine powder is obtained. More details of the process are reported elsewhere [7,8]. The obtained powder is annealed in a furnace in a thermal cycle with an oxygen flux enriched with 1 % ozone. The thermal cycle begins raising the temperature in 2 hours from ambient to 950 °C, then a plateau of 16 hours follows. Subsequently a 50 °C/h rate lowers the temperature to 550 °C and a second 10 hours plateau follows. The thermal treatment ends with a slow cool down with a rate of 50 °C/h to room temperature.

A single thermal treatment leads to the 123 phase with very few spurious materials as confirmed by X-ray and neutron diffraction analysis. The resulting $\text{Y}_1\text{Ba}_2\text{Cu}_3\text{O}_{7-\delta}$ shows an orthorhombic structure with the lattice parameters a, b, c respectively equal to 3.81, 3.88 and 11.67 Å. The oxygen content is about 6.8-6.9, as determined by neutron analysis [9]. The superconducting powder is pressed with an hydraulic press at 55 ton/cm² in pellets. The samples are sintered with the previously described thermal cycle leading to pellets with density of 5.5-5.9 gr/cm³ which show the presence of quite large crystals (300µm) with a preferential orientation [8]. The used samples have cylindrical shape with typical diameters ranging from 17 to 20 mm and a thickness between 2 and 6 mm.

In order to characterize the fabricated pellets, a.c. susceptibility measurements are carried out. In the usual magnetic susceptibility measurements a two coil system is used, where the first is the exciting and the second is the receiving coil. In this configuration, for superconducting materials, sometimes the samples are a separating surface between the two coils; otherwise the material is the core of the receiving coil. Small susceptibility variations are better measured by three coil bridge configurations [10]. Because thermal cycling may generate small impedance variations, then for high sensitivity measurements the coils should remain at constant temperature, while the sample temperature changes from 4.2K to 300K. In this case the thermal insulation reduces the volume available for the sample inside the coil, so that the signal reduces significantly. For frequency dependent susceptibility measurements, in which metallic parts must be avoided, the thermal insulation made by using plastic materials further reduces both the sample volume and the detected signal. Moreover the frequency dependence of the bridge balance makes difficult the use of the three coil configuration. For our purpose in the optimization of the fabrication method a large number of samples must be measured for a first screening. Moreover the signal generated by the complete shielding of a sintered pellet is large enough to allow the use of a simple apparatus. In this apparatus a single coil surrounding the sample is used and the temperature dependence of the self coil inductance is measured. The coil is wound on an insulating reel to avoid eddy currents and placed away from conducting materials. The

self inductance is measured by a LCR meter (LCR HP4262A). The meter sensitivity optimization suggested the use of a $990\mu\text{H}$ coil obtained by winding 180 turns of twice-glazed $200\mu\text{m}$ copper wire. The reel groove depth is 6 mm, the coil internal diameter is 22 mm and its length is 6 mm. The a.c. magnetic field values generated by the coil, because of the intrinsic limits of the LCR meter HP4262A, are 8, 2, 0.2 Gauss respectively for 120, 1K and 10K Hertz.

For a better sample characterization, in order to detect both χ' and χ'' , the two coil configuration is necessary, where the previous single coil system has been upgraded by a second external coaxial coil. This exciting coil, wound on an insulating reel, is 90 mm long, with an internal diameter of 35 mm and a self inductance of 35 mH. The coil is driven by a home made current generator able to give a.c. currents with an amplitude between 0 and 50 mA, constant for frequencies ranging from 0 to 100 KHz. This generator is driven by a function generator (Hewlett Packard model HP8116A). The real and imaginary part of the voltage drop across the receiving coil, has been measured by a Lock-In Amplifier (EG&G model 5208).

The measurements are generally done in presence of the earth's local magnetic field with a magnitude of about 0.5 Gauss.

In our measurements the sample is in thermal equilibrium with the coil, while the system is almost thermally insulated from the external world. The temperature is measured by a silicon diode (Lake Shore model DT470) in thermal contact with the sample. The insert, initially cooled at 77K, drifts slowly (about 1K/min) toward room temperature. The temperature pickup is connected to a temperature controller (Lake Shore model DRC91c).

All measured quantities are recorded by a computer acquisition system through the HPIB bus.

EXPERIMENTAL RESULTS

With our susceptometers, and in particular in the single coil configuration, the significant quantity, $L_s(T)$, proportional to the flux expulsion, is equal to the difference between the temperature dependent coil inductance values $l_v(T)$ and $l_s(T)$ respectively, measured in the absence and in the presence of the sample in the coil.

$$L_s(T) = l_v(T) - l_s(T) \quad (3)$$

In this way the spurious temperature dependence of the coil inductance are eliminated. For our coils and sample geometry, it is not easy to compute the signal generated by the complete magnetic shielding of samples. For simple geometries, in order to get an absolute calibration of the apparatus corresponding to the 100 % shielding, several cylindrical lead samples with different diameters and heights have been measured at the liquid helium temperature. These measures were interpolated so that the complete shielding signal, as function of the dimensions, is known.

In case of cylindrical superconducting samples with infinite length the surface shielding currents are completely insensitive to the presence of voids or non superconducting regions deeper than the penetration depth. On the contrary, for samples with a geometry similar to our sintered pellets, because of the large demagnetization coefficient, the shielding effect is weakly dependent on the presence of macroscopic holes in the sample.

For samples with irregular geometry, the absolute calibration is hard to obtain. In these cases, in order to understand if the observed signal corresponds to a complete shielding, the frequency dependence of $L_s(T)$ is studied. Indeed shielding currents in normal metallic samples show a frequency dependence, while no frequency dependence is observed in the superconducting state: for example see the insert of Fig. 5 and the following discussion.

In this way, as suggested by McCallum *et al.*, [2] the frequency dependence of the shielding currents is a clear method for detecting the presence of normal phases. In particular for high T_c sintered pellets in the presence of non superconducting materials, this method can discriminate between normal and insulating phases.

In order to verify the effectiveness of the ozone enriched oxygen atmosphere used in all thermal treatments, several samples with the same dimensions were made using the same fabrication procedure but respectively with or without the use of ozone. The comparison between the two kinds of samples was performed using the previously described single coil insert and the LCR bridge. The obtained behaviour is shown in Fig. 4 where the improvement obtained by the use of ozone is remarkable.

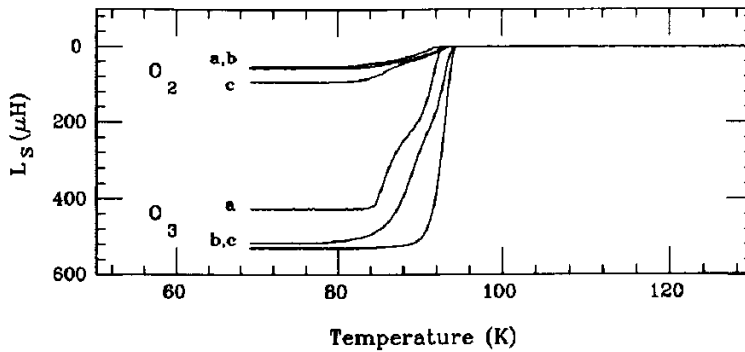


Fig. 4. Comparison between $L_s(T)$ for ozone and oxygen made samples measured at different frequencies with the corresponding amplitudes of the a.c. magnetic field: a) 120 Hz, 8 Gauss, b) 1 KHz, 2 Gauss, c) 10 KHz, 0.2 Gauss. In our calibration $530\mu\text{H}$ corresponds to the 100 % shielding value.

In Fig. 4, at the smallest magnetic field, the ozone made sample shows the 100 % shielding, obtained by a lead sample calibration, just 5K below the transition onset. Increasing the magnetic field the shielding, as expected, decreases and at 77K it is not able to reach the complete shielding. The ozone absolute shielding values are more than five time better than for the oxygen made samples because of both a larger effective superconducting region volume and a shorter effective penetration depth λ_{eff} . Moreover the shielding of the ozone made sample lowers only for magnetic fields greater than 1 Gauss, whilst the oxygen made sample degrades for much lower fields. In this way the behaviour

of the oxygen made sample at 1 and 8 Gauss are similar. The temperature and field dependence of the signal proves a much better coupling of the superconducting grains in the ozone samples: at 77K and for small fields the macroscopic transport currents are high enough to erase the granular structure.

For the study of the frequency dependence of the shielding effect our LCR meter cannot be used because only three frequency and current values are available, so that it was replaced by the lock-in amplifier and the previously described current generator. In this experimental configuration we have measured at 77K the frequency dependence of the shielding in the frequency range 120Hz - 10KHz at different a.c. fields, respectively for an ozone sintered pellet, ozone pressed powders and an oxygen sintered pellet. In particular Fig. 5 shows the $\Delta L_f\%$ as a function of the frequency f , where $\Delta L_f\%$ is defined as the variations of $L_s(f)$ respect to the measured value at the lowest frequency i.e.

$$\Delta L_f\% = \left[(L_s(120) - L_s(f)) / L_s(120) \right] \times 100 \quad (4)$$

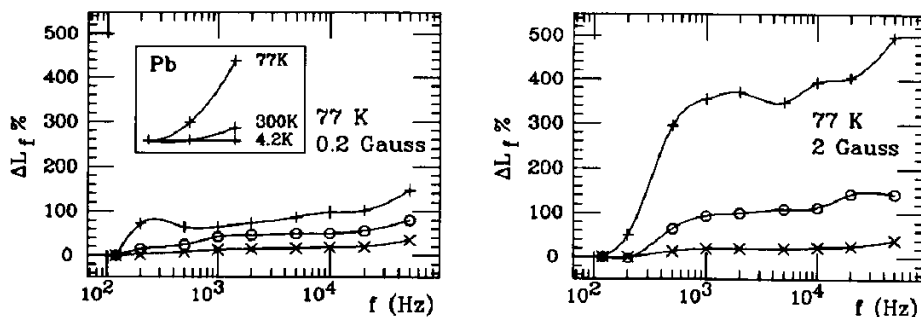


Fig. 5. Frequency dependence of $\Delta L_f\%$ as function of the frequency for two different fields. (+ Oxygen made pellet, x Ozone made pellet, o Ozone powder).

For comparison the insert of Fig. 5 reports the measurements performed on a lead sample respectively in the normal and in the superconducting state which follow the expected behaviour: i.e. the complete shielding effect in the superconducting state is frequency independent while in the normal state a large frequency dependence is observed; at low frequency this dependence increases as the conductance increases. The behaviour of the ozone made sample in the superconducting state is very close to the ideal behaviour; in comparison the oxygen made sample shows a much greater frequency dependence indicating the presence of small normal regions which interrupt the superconducting loops.

In order to analyse the samples in more detail the field and temperature dependence of both the real and imaginary parts of the susceptibility have been studied with the lock-in amplifier and the two coil system.

In order to improve the sample quality an oxygen atmosphere with more ozone has been used. The Fig. 6 A,B reports the transition of our best sample. The sample at 0.2 Gauss and 120Hz shows a transition width less than 1K. Both in the real and imaginary parts of the susceptibility it is impossible to distinguish the isolated grain transitions from the establishment of the grain coupling. In comparison Fig. 6 C shows the behaviour of the real part usually reported elsewhere and described in Fig. 3. In this case it is possible to distinguish between the grain transitions and the superconducting link activation.

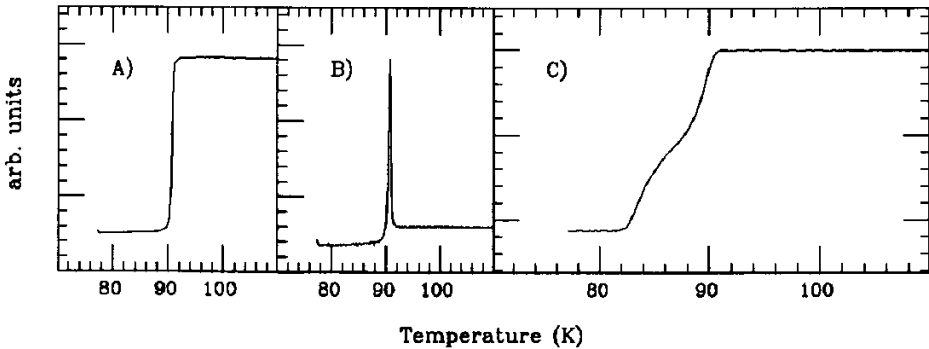


Fig. 6. Real A) and imaginary B) part of a low field transition ($H = 0.2$ Gauss; $f = 120$ Hz) together with the real part of a typical high field transition C) where the grains and the junctions contributions are easily separated ($H = 8$ Gauss; $f = 120$ Hz).

The behaviour of our best samples measured with a 5 Gauss a.c. magnetic field and for two different frequencies is reported in Fig. 7. As expected the transition width enlarges but the complete shielding is obtained 5K below T_c in both cases. On the contrary while at the 1KHz it is not possible

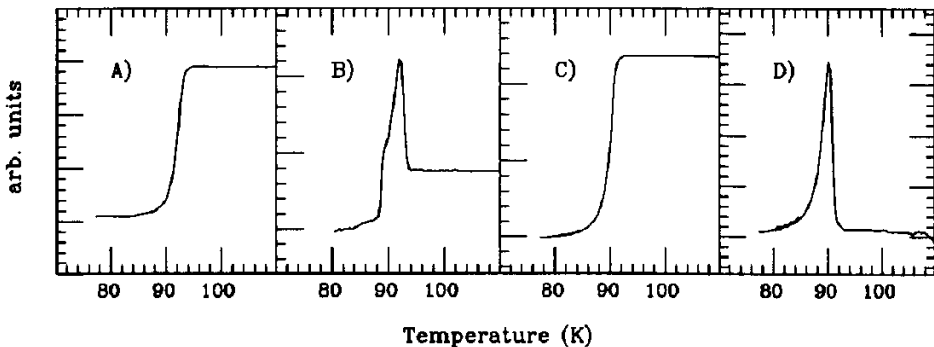


Fig. 7. Real and imaginary part of the high field transition for our best ozone made sample measured with an a.c. magnetic field of 5 Gauss. (A and B, $f = 120$ Hz); (C and D, $f = 1$ KHz).

to distinguish between grains and intergrain junction transitions (Fig. 7 D). At 120 Hz the presence of a shoulder in the imaginary part (Fig. 7 B) allows to infer the existence of the two transitions. The previously reported behaviour can be easily explained using the model reported in Fig. 1. In fact the presence of very small resistive regions on the superconducting loops can generate quite large current decay times. High enough frequency values do not allow the superconducting current decays. As a consequence the magnetic flux cannot penetrate into the sample and in practice there is no hysteresis formation in the magnetization plots.

CONCLUSIONS

We believe that the use of the pyrolysis allows the best mixing of the components, and the use of an ozone enriched oxygen atmosphere leads to improvements of the produced sample quality. A good mixing determines a drastic reduction of localized non stoichiometric defects, which generate many small non superconducting regions corresponding to a large value of the effective non superconducting volume. The use of ozone allows a better oxidation and a strong coupling of the superconducting grains. This fact is evident from both the comparison of the temperature dependent shielding values for complete shielding, and from the frequency behaviour of the shielding itself. The absence of a frequency dependent shielding can be a clear criterion for the verification of a complete shielding in all cases where is not possible to have a direct absolute calibration.

Up to now the effect of the ozone during the different steps of the fabrication process is not known in detail but the experimental data clearly show that the ozone improves the grain coupling and reduces the effective volume of the non superconducting phases. More detailed analysis on the process are scheduled for the future.

REFERENCES

- 1 V. Calzona, M.R. Cimberle, C. Fedreghini, M. Putti and A.S. Siri, Physica C, **157** (1989) 425.
- 2 R.W. McCallum, W.A. Karlsbach, T.S. Radhakrishnan, F. Pobell, R.N. Shelton and P. Klavins, Solid State Commun., **42** (1982) 819.
- 3 A. Barone and G. Paterno', Physics and applications of the Josephson Effect, Wiley, New York, 1982.
- 4 U. Gambardella, G. Paterno', C. Alvani and S. Casadio, Vuoto, **XVIII** (1988) 218.
- 5 T. Takabatake, M. Ishikawa and T. Sugano, Jap. J. Appl. Physics, **26** (1987) L1859.
- 6 J. Flokstra, G. J. Gerritsma, D.H.A. Blank, and E.G. Keim, Proc. of the European Workshop on: High Tc Superconductors and Potential Applications, Genoa, 1-3 Jul 87, pg. 429.
- 7 F. Celani, R. Messi, S. Pace and N. Sparvieri, Il Nuovo Saggiatore, **4** (1988) 7.
- 8 F. Celani, L. Fruchter, C. Giovannella, R. Messi, S. Pace, A. Saggese and N. Sparvieri, IEEE trans. on Magn., **25** (1989) 2348.
- 9 A. Balzarotti, M. De Crescenzi, N. Motta, F. Patella and A. Sgarlata, Phys. Rev. B, **38** (1988) 6461.
- 10 J. Flokstra, G. J. Gettitsma, H. J. M. Krouwel and L. C. van der Marel, J. Phys. E: Sci. Instrum., **13** (1980) 1071.